RSC Advances

PAPER

View Article Online
View Journal | View Issue

Cite this: *RSC Adv.*, 2017, **7**, 19565

Micro-patterned titanium coatings with a grid-like structure doped with vancomycin against bacteria and affecting osteogenic differentiation

Guangchao Wang, †[a] Hao Zhang,†[a] Qianyun He,[a] Dake Tong,[a] Chen Ding,[a] Peizhao Liu,[a] Zequan Zhang,[b] Youtao Xie*[b] and Fang Ji*[a]

Titanium and its alloy are widely used in orthopedic surgery. However, Ti implant-associated infections continue to be the primary cause of titanium implant failure. The present study aimed to investigate the effects of micro-patterned titanium coatings doped with vancomycin on antibacterial activity and osteogenic differentiation and to improve the bioactivity of the inert titanium. A micro-pattern was fabricated on titanium, then calcium phosphate bone cement and vancomycin were doped on the micro-patterned titanium with a grid-like structure on the surface for anti-bacterial activity. *Staphylococcus aureus* and methicillin-resistant *S. aureus* were applied to investigate the bacterial adhesion and biofilm formation at 6 h, 24 h, 3 d and 7 d using the spread plate method, confocal laser scanning microscopy and scanning electron microscopy. Human bone marrow mesenchymal stem cells were used for investigating the cell biocompatibility and osteogenic differentiation of the titanium substrate. The result showed that vancomycin could release on the micro-patterned titanium within 6 d and the burst release was reduced. The calcium phosphate bone cement–vancomycin doped micro-patterned titanium with a grid-like structure could resist bacterial infection for 7 d. The osteogenic differentiation of human bone marrow mesenchymal stem cells with the titanium substrate was analysed by the alkaline phosphatase activity and alizarin red staining semi-quantitative analysis of the micro-patterned Ti (Tp) and the CPC–VCM doped micro-pattern Ti (TV), and was demonstrated to be higher than that of the Ti without patterning (T0) at 7 d and 14 d, respectively. The real-time PCR also indicated that the Tp and TV upregulated human alkaline phosphatase, type I collagen at 7 d and osteopontin were also upregulated after incubation for 14 d. The *in vitro* study indicated that calcium phosphate bone cement–vancomycin doped on the micro-patterned titanium with a grid-like structure surface is a promising approach to fabricate multi-biofunctional titanium against bacteria and promoting osteogenic differentiation.

Received 10th December 2016
Accepted 13th March 2017

DOI: 10.1039/c6ra27996a

rsc.li/rsc-advances

Introduction

Despite the wide application of orthopedic implants in the treatment of various diseases, failure of orthopedic implants remains a problem. The main causes of failure of orthopedic implants are aseptic loosening and infection.[1,2] The orthopedic prosthesis, once implanted, will encounter a risk of occurrence of microbial infection, especially in open fracture fixation and arthroplasty operations.[3,4] Therefore, developing novel orthopedic implants to avoid infection is still an urgent need. In recent years, among various antibacterial metal coatings such as hydrogel coatings,[5] plasma coatings,[6] silver coatings,[7] *etc.*, titanium (Ti) and its alloys have attracted scholars' attention and become popular for orthopedic implants in many fields, such as hip and knee prosthesis, fixation, and dental implants. As with other orthopedic implants, the ultimate goal of fabricating the orthopedic Ti implant is also to avoid complications post-implant, and fabricating an anti-bacterial Ti implant is the primary goal in the prophylaxis of Ti implant-associated infection.

The surface properties of an implant are correlated with their biological behavior. A rough surface promotes cell adhesion, proliferation, and contact osteogenesis.[8] Surface modification of Ti is a critical approach for improving the biocompatibility of Ti. The physicochemical surface properties of Ti, including the chemical composition, hydrophilicity, surface roughness, and surface pattern, could affect the cellular response to the Ti surface and ultimately the *in vivo* performance.[9] The micro-

[a]*Department of Orthopedics, Changhai Hospital, The Second Military Medical University, No. 168 Changhai Road, Shanghai 200433, China. E-mail: doctorjif@126.com; Fax: +86-21-31161696; Tel: +86-21-31161696*

[b]*Key Laboratory of Inorganic Coating Materials, Shanghai Institute of Ceramics, Chinese Academy of Sciences, Shanghai 200050, China. E-mail: xieyoutao@mail.sic.ac.cn; Fax: +86-21-52412990; Tel: +86-21-52412990*

† These authors contributed equally to this work.

patterned surfaces on the implant could provide physical differentiation cues to human bone marrow mesenchymal stem cells (hBMSCs).[10,11] Our previous study indicated that the micro-patterned coatings with a grid-like structure on titanium could enhance the early cellular responses and up-regulate the osteogenic-related genes.[12] However, the simple surface modification of Ti could directly improve the biocompatibility of Ti, such as promoting BMSCs adhesion and proliferation or promoting osteogenic differentiation, and not prove lethal to the bacteria in contact with the surface.

Two main approaches have been proposed for the biofunctionality of Ti for anti-bacterial activity, which is dependent on the ability of the Ti implant surface to locally deliver the anti-bacterial agents. The implant surface is mainly divided into two parts: the passive and active antibacterial Ti surfaces.[13] Passive antibacterial Ti surfaces refer to those that can inhibit bacterial adhesion or kill the bacteria when in contact with the surface. On the other hand, the active antibacterial Ti surface can locally deliver the anti-bacterial agents and kill the bacteria around the Ti implant.[14] The passive coating on the Ti surface is an effective approach to inhibit bacterial adhesion and biofilm formation on the Ti surface. It can burst release antibiotics and rapidly kill the surrounding bacteria in the critical duration of prophylaxis for the implant-associated infection, which is 4–6 h post implantation surgery.[15] Furthermore, the local controlled release of the antibiotic can avoid the complication of systemic administration, thereby representing a promising approach to biofunctionalize Ti for anti-bacterial activity.

Calcium phosphate bone cement (CPC) is a promising candidate for bone regeneration owing to its great bone affinity, injectability, and *in situ* hardening properties. CPC is also an excellent antibiotics carrier due to its self-setting *in vivo* and injectability.[16] The antibiotic- (gentamicin and vancomycin) loaded cement showed a controlled release within several weeks and high antimicrobial potency against *S. aureus*.[17] The Ti implant coating with CPC can improve the bone-implant osteointegration.[18] Thus, the CPC coating on Ti can not only function in the loading of antibiotics for anti-bacterial activity but also improve the bone-implant osteointegration *in vivo*.

A perfect Ti implant should perform two biofunctions: prophylaxis to bacterial infection and promotion of osteogenesis. The approach to biofunctionalization of Ti should take these two biofunctions into account.[19–22] In the present study, we aimed to fabricate an antibacterial and osteogenic Ti coating. A micro-pattern was fabricated on Ti for improving the hBMSCs' responses such as cell adhesion, spreading, proliferation, and osteogenic differentiation. We also investigated the feasibility of doping CPC and vancomycin (VCM) on the micro-patterned Ti surface for anti-bacterial activity.

Materials and methods

We used 3 samples for every experiment, and all experiments were conducted in triplicate. Ti6AL4V (Ti alloy, $\Phi 10 \times 2$ mm) and all of the Ti samples were sterilized *via* ultraviolet (UV) irradiation for the cell experiment. Other reagents and kits used were: fetal bovine serum (FBS; Gibico, Australia), trypsin-ethylenediaminetetraacetic acid (EDTA, Hyclone), CCK-8 Kit (Donjindo, Japan), LIVE/DEAD® BacLight. Bacterial Viability Kits (Molecular Probes), 4′,6′-diamidino-2-phenylindole (DAPI, Sigma-Aldrich), rhodamine phalloidin (Amanita phalloides) alizarin red, dexamethasone, ascorbic acid, β-glycerol phosphate (Sigma-Aldrich), ALP Staining Kit, ALP Quantitative Kit (Beyotime Biotechnology, China), Pierce™ BCA Protein Assay Kit (ThermoFisher), *Staphylococcus aureus* (ATCC 25923) and methicillin-resistant *S. aureus* (MRSA, ATCC, 43300).

Preparation of a micro-patterned Ti coating with VCM loading and characterization

The Ti substrates ($\Phi 10$ mm $\times$ 2 mm and $\Phi 34$ mm $\times$ 2 mm) were grit blasted, ultrasonically washed with ethanol and dried prior to plasma spraying. Pure Ti powder was sprayed onto the treated substrates using an atmospheric plasma spray system; the parameters are listed in Table 1. For generating patterns of various sizes, Ti meshes with different dimensions were used to block the particles. The Ti particles were only allowed to be deposited within the open spaces, and the micro-patterned coating (denoted Tp; the Ti samples without patterns are denoted T0) was ultimately generated after the removal of the Ti wire mesh.

The Tp samples were sterilized by high-pressure steam and drying in a desiccator. The solidified CPC and VCM were mixed according to the mass ratio 160 mg : 1 g,[23] followed by the addition of the curing liquid with complete stirring for 30 s. The samples were denoted CPC–VCM. Then, the Tp sample and CPC–VCM were mixed as a solution under vacuum control at 0.06 MPa, creating the vacuum while applying the CPC–VCM on the Tp surface for 3 min and the CPC–VCM mixed solution into the coating pore. Subsequently, the sample was removed. After full curing for 24 h, the surface was polished smooth for the drug-loading pattern sample layer (the Ti samples are denoted TV). The weights of the Ti and drug-loading Ti were estimated and the amount of VCM on the Tp was calculated.

Drug release characterization

The VCM released from the interconnected structure of the Ti coating was determined from samples individually immersed in 1 mL PBS on a 24-well plate at room temperature and agitated at 70 rpm. After 15 min, 30 min, 1 h, 2 h, 4 h, 8 h, 1 d, 2 d, 4 d, and 6 d, 1 mL of solution was sampled, and the PBS was replenished with fresh solution. The samples were stored at −20 °C. The VCM concentration was estimated using ultraviolet spectrophotometry (Inesa Analytical Instrument Co., Ltd, Shanghai,

Table 1 Plasma spraying parameters

Parameters	Values	Units
Current	650	A
Voltage	72	V
Spray distance	140	mm
Ar gas flow	40	slpm
H_2 gas flow	10	slpm

China) at 237 nm. A standard curve of VCM concentrations was adopted to determine that in the PBS.

In vitro antibacterial assay

Spread plate method. Since *Staphylococci* are the most common micro-organisms causing orthopedic implant infections, *S. aureus* and MRSA were chosen to investigate the extent of bacterial colonization on the T0, Tp, and TV. *S. aureus* and MRSA were inoculated in tryptone soy broth (TSB) with agitation (150 rpm) at 37 °C for 3 h before the antibacterial experiment. The bacterial density was adjusted to 1×10^6 colony-forming units (CFU) mL^{-1}. The antibacterial activity was measured using the method described elsewhere.[24] Briefly, various Ti (T0, Tp, TV) samples were placed in 24-well plates and incubated for 6 h, 24 h, 72 h, and 1 week with bacteria in TSB medium under agitation (150 rpm) at 37 °C. Each sample was then rinsed with PBS to remove any non-adherent bacteria. The adherent bacteria on each Ti sample were detached by ultrasonication for 20 min in a 150 W ultrasonic bath. After serial dilutions, the number of viable bacteria in the sample suspensions was determined as the number of CFUs. The number of CFUs on the TSA plate was counted visually for quantitative analysis. The bacterial counts were then normalized to log-reduction.

Characterization of the antibacterial property with confocal laser-scanning microscopy (CLSM) and scanning electron microscopy (SEM). After 6 h, 24 h, 72 h, and 1 week, the Ti substrate from each group was rinsed with sterile PBS to remove any non-adherent bacteria and then transferred to a new 24-well plate. Subsequently, the Ti samples were stained using a LIVE/DEAD BacLight bacterial viability kit, according to the manufacturer's instructions. The samples were rinsed twice in sterile PBS and analyzed with a CLSM (Leica TCS SP2, Germany), wherein the live bacteria appear green and the dead bacteria appear red.

The antibacterial property of each Ti substrate was also characterized using SEM. In brief, each Ti substrate was incubated with bacterial suspensions of 1×10^6 CFU mL^{-1} in TSB in a 24-well plate. After 6 h, 24 h, 72 h, and 1 week, each of the Ti samples was fixed in 2.5% glutaraldehyde for 24 h at 4 °C, washed with PBS, and dehydrated through a gradated series of ethanol (50%, 70%, 80%, 90%, and 100%). The samples were subsequently freeze-dried, sputter-coated with gold, and observed using a SEM (JEOL, JSM-6700F, Japan).

Cell adhesion, proliferation, and morphology. Human bone marrow mesenchymal stem cells (hBMSCs) were isolated clinically as described elsewhere.[25] All experiments were approved by the Ethics Committee of Changhai Hospital, Shanghai, China and performed according to the relevant laws and institutional guidelines of the Ethics Committee of Changhai Hospital. The cells were digested with trypsin, diluted to a density of 5×10^4 cells per mL, and then seeded (0.5 mL per well) onto the Ti samples placed in the 24-well plates. At 4 h, 8 h, 12 h, 1 d, 3 d and 5 d after seeding, each Ti sample was washed with PBS. Cell adhesion and proliferation were recorded using a CCK-8 assay. After 24 h of culturing, each Ti sample was fixed with 4% paraformaldehyde, permeabilized with 0.1% Triton X-100 for 15 min, and gently rinsed with PBS. The samples were then counter-stained in 4′,6′-diamidino-2-phenylindole (DAPI; 5 μg mL^{-1}) for 15 min to stain the nucleus. The cytoskeleton was stained with rhodamine-phalloidin for 30 min according to the manufacturer's protocol and then analyzed using a CLSM.

Osteogenic differentiation of hBMSCs on Ti substrates *in vitro*

ALP assay. ALP staining and activity were investigated as the early osteogenic differentiation markers. Briefly, each Ti sample was placed in a 24-well plate, and the hBMSCs were seeded on each specimen at a density of 5×10^4 cells per mL (1 mL per well). After 24 h, the medium was replaced with an osteogenic differentiation-inducing medium (10% culture medium containing 100 nM dexamethasone, 50 μM ascorbic acid and 10 mM β-glycerol phosphate). Following incubation for 7 d and 14 d, the ALP staining and activity were investigated using an ALP Quantitative Kit.

Alizarin red staining and semi-quantitative analysis. Extracellular matrix (ECM) mineralization was examined after *in vitro* culturing for 7 d and 14 d. The Ti samples were washed twice with PBS, fixed with 4% paraformaldehyde for 20 min, and then subjected to Alizarin red staining for 5 min. The excess stain was removed using 10% cetylpyridinium chloride, and the OD value at 620 nm was estimated for quantitative analysis.

Real-time PCR for the *in vitro* investigation of the osteogenesis of hBMSCs. For RNA extraction, the Ti substrate size was $\Phi 34 \times 2$ mm. The hBMSCs were seeded at a density of 5×10^4 cells per well and cultured in 6-well plates prior to the addition of Ti. After *in vitro* culturing for 7 d and 14 d, total RNA was isolated from each Ti sample using TRIzol (Invitrogen). The purity of the RNA was estimated quantitatively (NanoDrop ND-1000 Spectrophotometer). Subsequently, 1 μg RNA from each Ti sample was reverse transcribed into complementary DNA (cDNA) using the PrimeScript™ RT Kit. The osteogenic-related gene expression of the hBMSCs was quantified by real-time PCR on an ABI 7500 real-time PCR System (Applied Biosystems, USA) using a PCR kit. The comparative C_t-value method was used to calculate the relative quantity of human alkaline phosphatase (ALP), type I collagen (COL1), osteopontin (OPN), and osteocalcin (OC). The gene primers were obtained from Sangon Biotech and are presented in Table 2. The expression of the housekeeping gene glyceraldehyde-3-phosphate dehydrogenase (GAPDH) was used as an internal control. The $2^{-\Delta\Delta C_t}$ method was applied to analyze the data and all experiments were conducted in triplicate.

Statistical analysis. All of the data are expressed as mean ± standard deviation. One-way analysis of variance (ANOVA) was performed, and confidence intervals (CI) were determined using SPSS software (19.0) followed by the Student-Newman–Keuls test (SNK) to evaluate the differences between the groups. p-Values <0.05 were considered statistically significant.

Results

Characterization of the micro-patterned Ti coating and the VCM loading on the micro-patterned Ti coating

The surface morphology of the Ti substrates is shown in Fig. 1. The micro-patterned Ti (Tp) exhibiting a grid structure on the

Table 2 Primers used in the study

Osteogenesis gene	F	R
COL1	5′-CCTGAGCCAGCAGATCGAGAA-3′	5′-GGTACACGCAGGTCTCACCAGT-3′
ALP	5′-TTGACCTCCTCGGAAGACACTC-3′	5′-CCATACAGGATGGCAGTGAAGG-3′
OPN	5′-CTGAACGCGCCTTCTGATTG-3′	5′-ACATCGGAATGCTCATTGCTCT-3′
OC	5′-GGCGCTACCTGTATCAATGGC-3′	5′-TGCCTGGAGAGGAGCAGAACT-3′
GAPDH	5′-CCTGCACCACCAACTGCTTA-3′	5′-AGGCCATGCCAGTGAGCTT-3′

surface coincided with the substrate. For the CPC–VCM doping on the micro-patterned Ti (TV), several pores and particles were observed.

VCM loading and release

The total CPC–VCM loading on the Ti substrates was 660 ± 280 μg; according to the mass ratio, the total amount of VCM loading on the Ti substrates was 568 ± 241 μg. As shown in Fig. 2, the VCM burst release curve was curved inwards not curved outwards, which indicates that the CPC–VCM on the micro-pattern with a grid-like Ti coating could reduce the burst release of VCM. Furthermore, as shown in Fig. 2, the VCM release reached a plateau at day 6, which indicates that the VCM can locally control the release for 6 d.

Antibacterial property against planktonic bacteria

At each time point, T0 and Tp did not show any antibacterial properties against *S. aureus* and MRSA, while VCM displayed excellent antibacterial properties within 7 d, as we found fewer bacteria on the TV surface compared with on the T0 and Tp

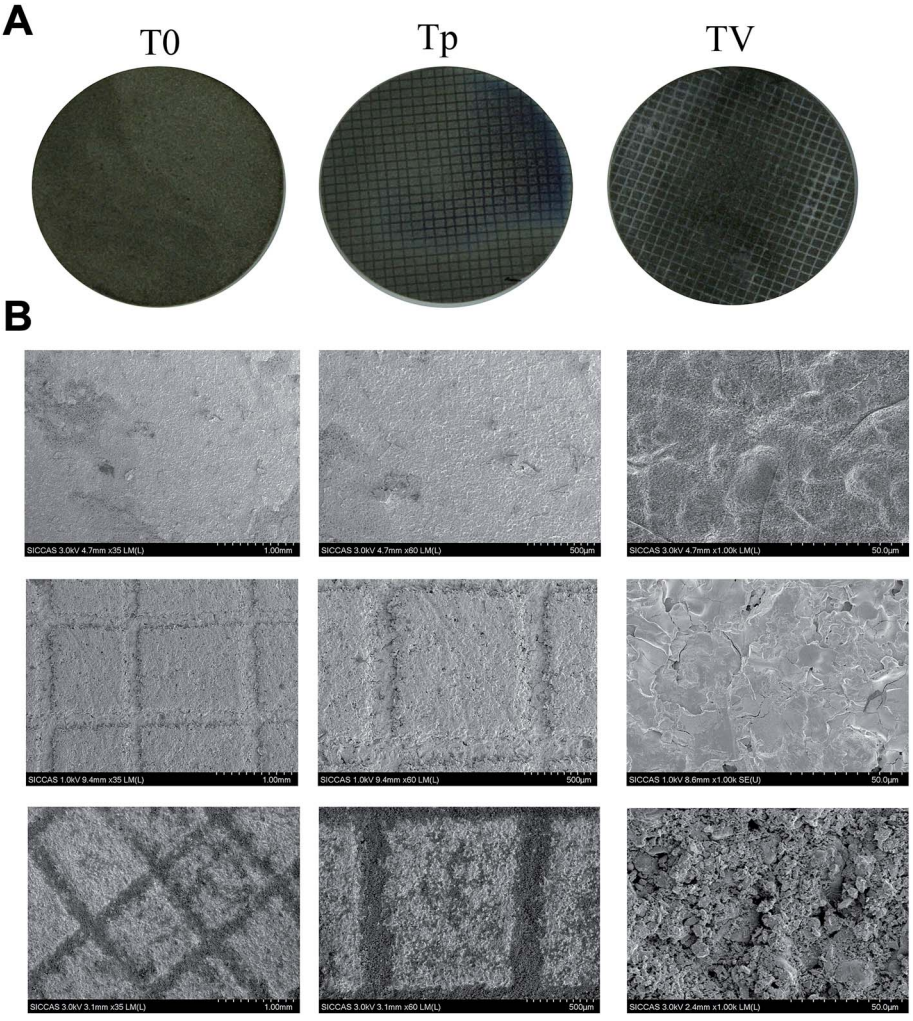

Fig. 1 (A) Characterization of the micro-patterned surfaces. (B) SEM images of the surface morphologies of the plasma-sprayed Ti coatings, micro-patterned Ti coating surface, and VCM-doped micro-patterned Ti coating.

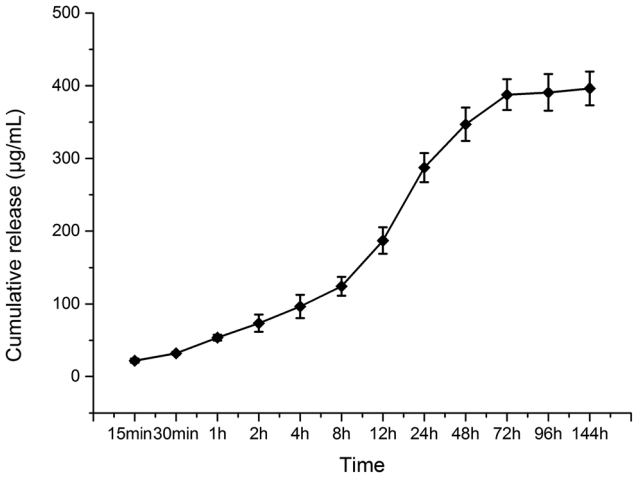

Fig. 2 Drug release from the micro-patterned Ti coating: burst release of VCM from the micro-patterned Ti coating and sustained controlled release of VCM from the micro-patterned Ti coating.

surfaces (Fig. 3). This result demonstrated that the TV can controlled release locally and keep its antibacterial property. The bacteria in the TV group were reduced by 1.79-log, 2.54-log, 2.71-log and 3.98-log compared to the T0 group at 6 h, 24 h, 72 h and 1 week, respectively, for *S. aureus*. In addition, they were reduced by 1.73-log, 2.56-log, 2.63-log and 3.07-log compared to the T0 group at 6 h, 24 h, 72 h and 1 week, respectively, for MRSA (Fig. 4).

CLSM and SEM

CLSM and SEM were used to further investigate the antibacterial properties of the Ti substrates. As shown in Fig. 5, after culturing on the Ti substrates (T0, Tp, TV) for 4 h, 24 h, 3 d, and 7 d, the green fluorescence intensity (denoting live bacterial colonies) on the Ti control increased, which indicated remarkable bacterial growth. Similar results were observed in the Tp group, whereas the green fluorescence intensity decreased on the bacteria cultured on the TV group, and the red fluorescence intensity (denoting dead bacterial colonies) increased. According to Fig. 6, large amounts of bacterial colonies were observed in the T0 and Tp groups at each time point, while fewer bacteria were observed in the TV group. These results indicate that the VCM released from the micro-patterned Ti could effectively kill the bacteria.

Cell adhesion and proliferation

A CCK-8 assay was used to assess the cell adhesion and proliferation of hBMSCs after being cultured on T0, Tp and TV for 4 h, 8 h, 12 h, 1 d, 3 d and 7 d. The results showed that after incubation for 4 h, 8 h and 12 h, the number of cells cultured on Tp and TV was significantly higher than that cultured on T0 ($p < 0.05$) (Fig. 7). These results demonstrated that the topography of the micro-patterned Ti could stimulate the adhesion and proliferation of hBMSCs.

CLSM to characterize the cell morphology

The morphology and distribution of hBMSC after 24 h of culturing on the Ti substrate were observed using CLSM. Actin filaments were stained red with phalloidin. Fig. 8 demonstrates that the hBMSCs attached on T0, Tp and TV, and spread into a fibroblast-like morphology.

hBMSC osteogenic differentiation

As shown in Fig. 9A, the ALP quantitative assay revealed that Tp had a higher ALP activity than pure T0 and TV, and no significant difference was observed between T0 and TV at day 7. On the other hand, at day 14, Tp displayed the highest ALP activity, and the TV group had a higher ALP activity than T0. The quantitative assay of ECM calcium deposition showed that Tp and TV exhibited a larger calcium deposition area than T0 after 14 d culturing. Moreover, Tp displayed greater calcium deposition than TV. No significant difference was observed between T0, Tp and TV at day 7 (Fig. 9B).

Real-time PCR for the detection of the genes correlated with osteogenic differentiation

The expression of the genes related to osteogenesis, including ALP, COL1, OPN and OC, in the cells cultured on pure T0, Tp and TV for 7 d and 14 d were quantified by real-time PCR, and the results are shown in Fig. 10. The Tp and TV groups upregulated the gene expressions (COL1, OPN and OC) in hBMSCs, after incubation for 7 d. The cells on Tp expressed the highest mRNA level of ALP, COL1 and OC among the three groups at day 7. At day 14, the cells on Tp and TV expressed higher mRNA levels of OPN and OC than T0. The expressions of ALP and COL1 on Tp were also greater than those on T0 and TV.

Discussion

Peri-implant infection and loosening are the two most significant complications of Ti implant surgery. Therefore, fabrication of an ideal Ti implant to prevent such complications is essential. Biofunctionalization of Ti for anti-bacterial activity and promoting osteogenic differentiation is the ultimate goal of fabricating a perfect Ti implant.[21,26,27] In the present study, a micro-pattern coating with a grid-like structure was fabricated on Ti for improving the hBMSCs' responses such as cell adhesion, spreading, proliferation and osteogenic differentiation. Then, the micro-patterned Ti coating with the grid-like structure was doped with CPC and VCM for anti-bacterial activity. *In vitro* bacteria co-cultures were established for 4 h, 24 h, 3 d and 7 d time points. These revealed that micro-patterned Ti doped with CPC and VCM exerts a significant effect on bacterial adhesion and biofilm formation compared to T0 and Tp.

The biofilm formation on the Ti implant is composed of several steps including bacterial adhesion on the implant surface followed by the proliferation of the bacteria and biofilm formation. The biofilm consisting of the extracellular polymeric substances, after formation, results in peri-prosthetic infection, rendering the peri-implant infection treatment more difficult.[28] The period of 4–6 h post-implant surgery has been identified as

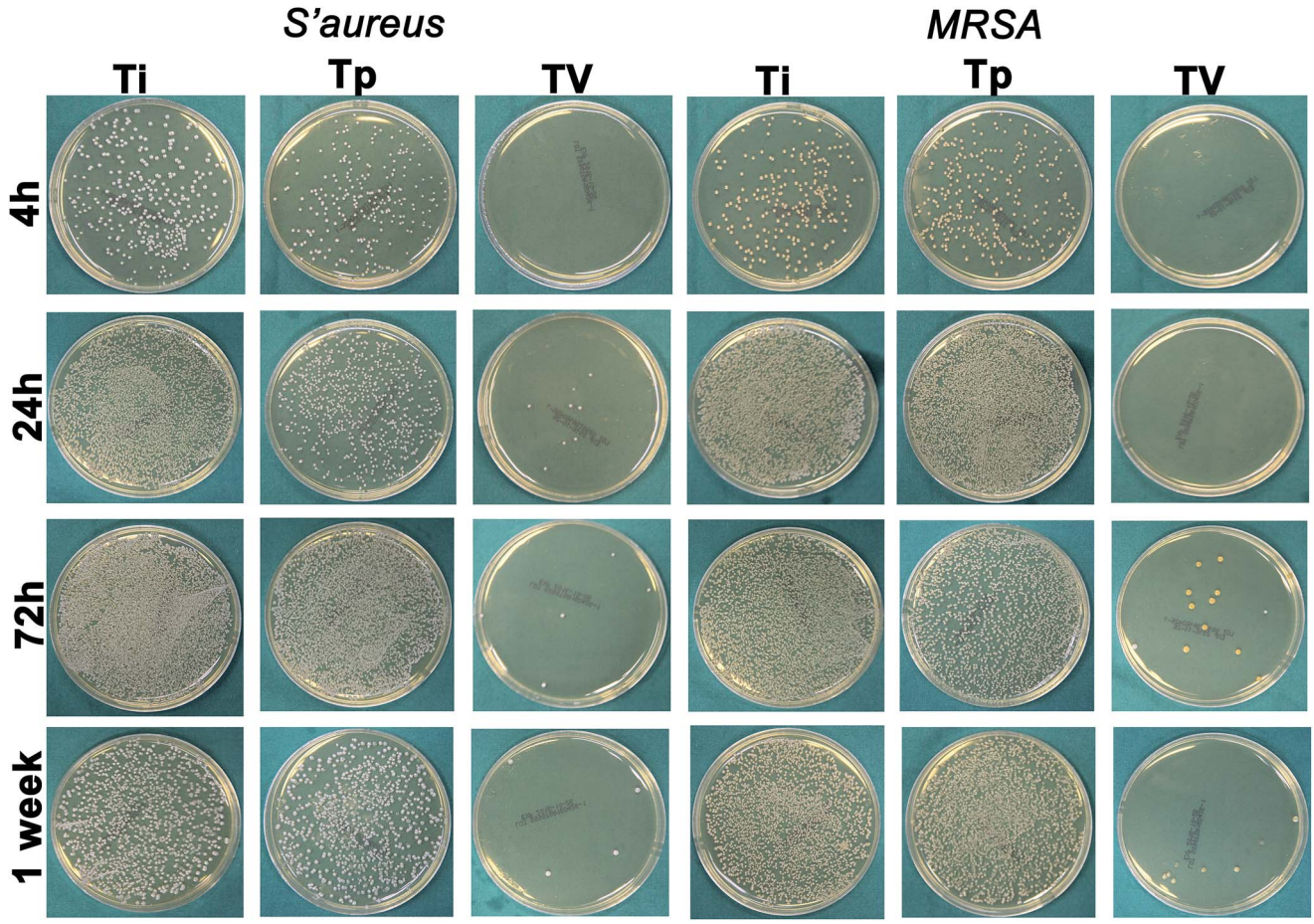

Fig. 3 Spread plate method to observe the bacteria CFU on the Ti substrate at 4 h, 24 h, 72 h and 1 week. The bacteria count was diluted to 10^3 for 24 h counting and diluted to 10^4 for 72 h and 1 week counting. *S. aureus* 25923 and MRSA were used for the antibacterial assay. Compared to the Tp and T0 substrates, the bacterial colonies on the TV group were fewer. A large number of bacterial colonies were observed on the T0 and Tp groups at each time point.

the "decisive period", thus, inhibiting the bacterial adhesion in the 4–6 h after the implant surgery could inhibit the biofilm formation in the long-term.[22,29–31] CPC–VCM on this coating could control the release of VCM within 7 d. These results revealed the superiority of CPC doped on the Ti surface while acting as an antibiotic carrier, which can sustain the release of

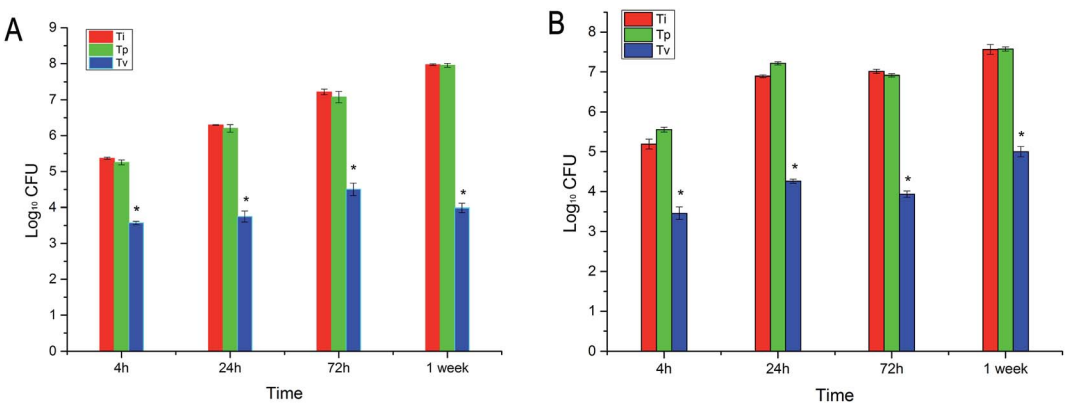

Fig. 4 Spread plate method to characterize the bacterial counts on each Ti surface (T0, Tp and TV). (A) Each time point bacterial (*S. aureus*) count on the TV group was significantly lower than that of the T0 and Tp groups ($p < 0.05$); no significant difference was observed between the T0 and Tp groups ($p > 0.05$). (B) At each time point the number of MRSA on the TV group was significantly lower than that of the T0 and Tp groups ($p < 0.05$); no significant difference was observed between the T0 and Tp groups ($p > 0.05$). The log of the number of bacteria was used on the standardization plot.

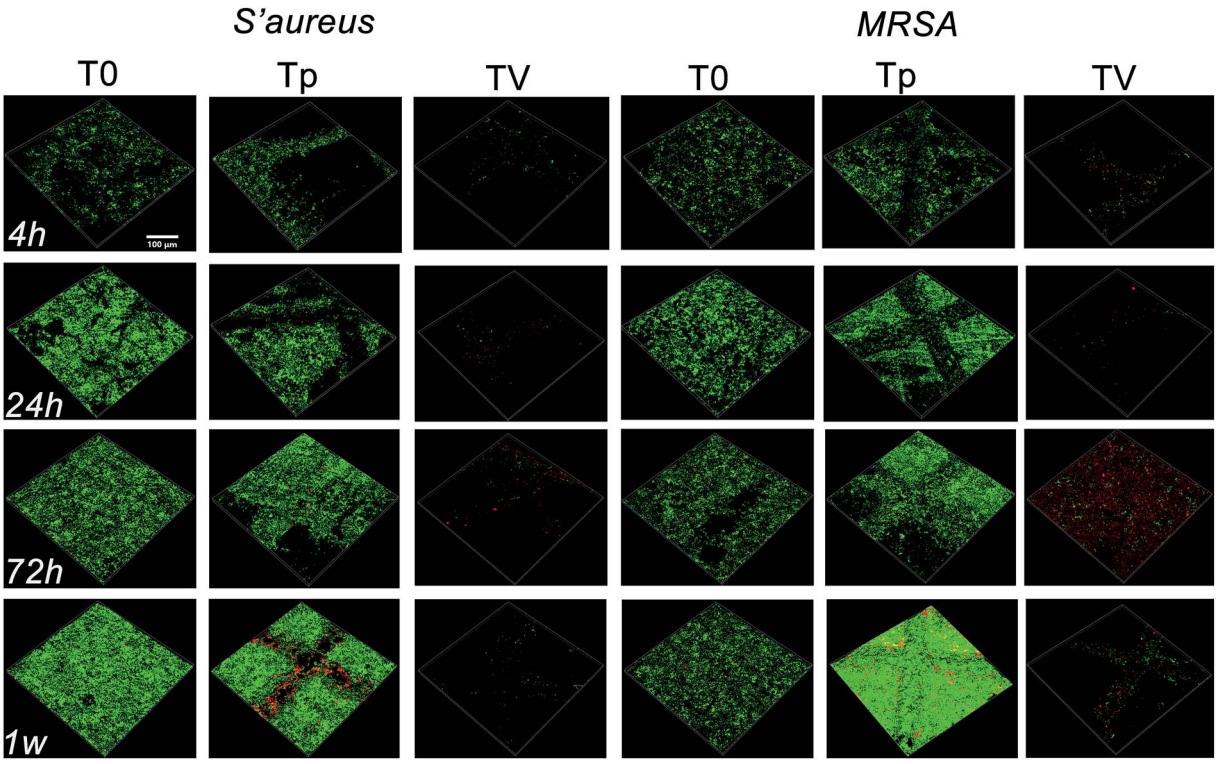

Fig. 5 CLSM to observe the bacterial growth on the Ti substrates at 6 h, 24 h, 72 h and 1 week. At 4 h, a large number of viable bacteria (stained green) were observed while little green fluorescence was seen in the TV group. At 24 h, 72 h and 1 week, the green fluorescence was enhanced, which indicated the formation of a biofilm. While less green fluorescence was observed in the TV group, the red fluorescence increased.

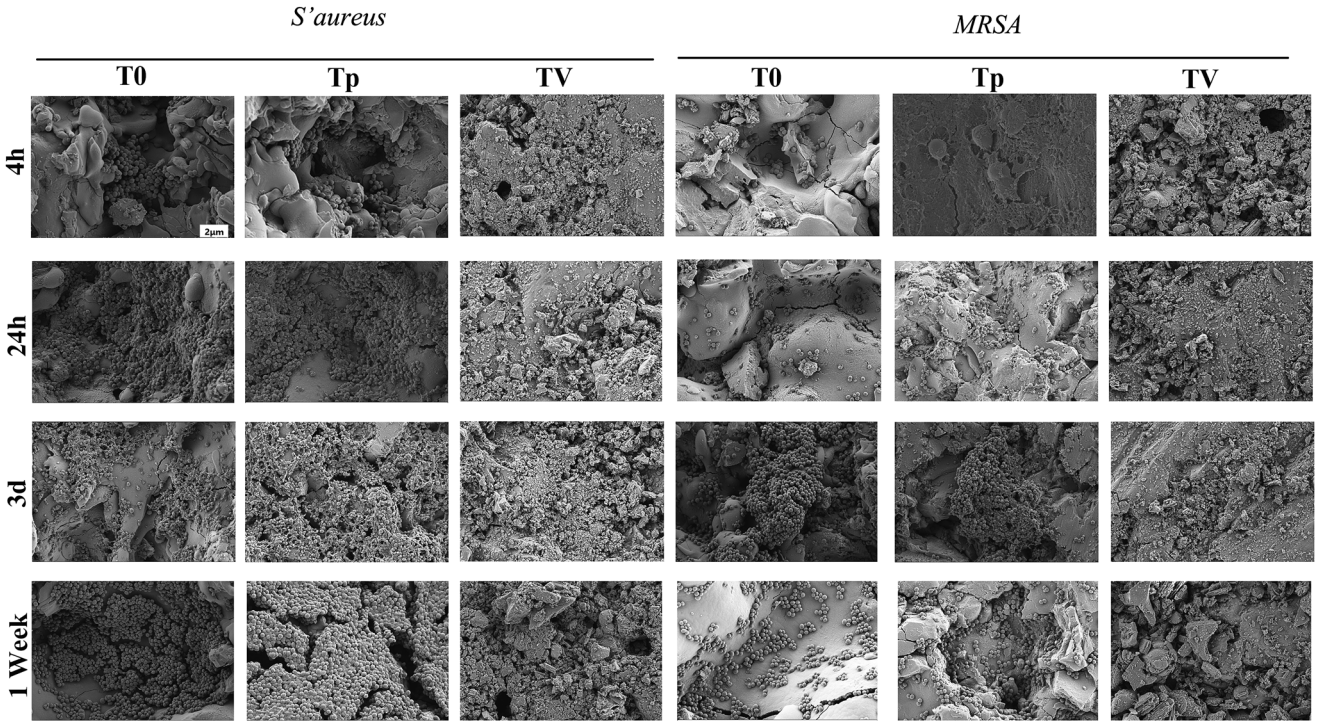

Fig. 6 SEM to characterize the bacterial colonization on various Ti substrates after co-culturing for 6 h, 24 h, 3 d and 7 d.

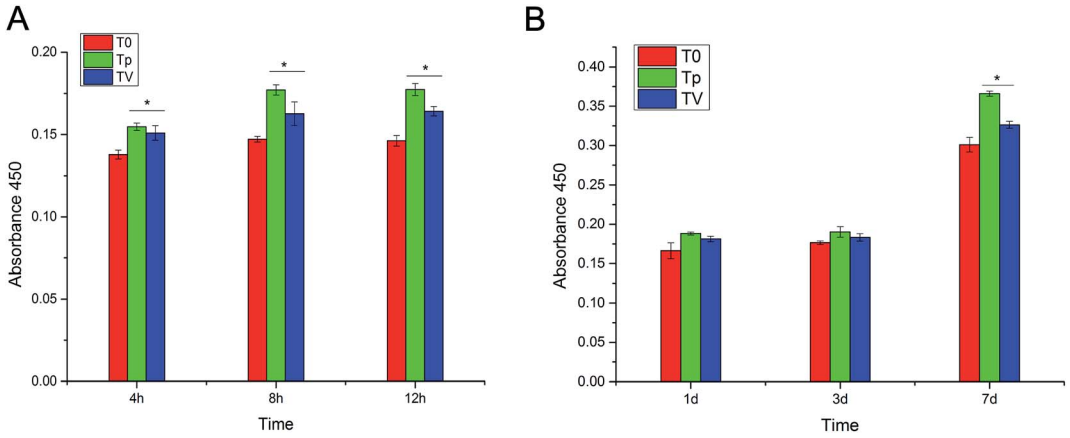

Fig. 7 CCK-8 assay to investigate the hBMSC cell adhesion and proliferation on various Ti substrates (T0, Tp, and TV). (A) Adhesion experiment results showed that Tp and TV could promote cell adhesion at each time point; loading of vancomycine on Tp did not affect the cell adhesion. (B) Cell proliferation was not apparent after 3 d of culturing; however, at day 7, the cell proliferation on Tp and TV was significantly higher than that of T0. The results show that the loaded VCM and TV can promote cell proliferation.

VCM locally. The released VCM retains its bactericidal properties, and the burst release of VCM could ensure the efficient killing of the bacteria surrounding the Ti implant, thereby preventing biofilm formation. Our results also showed that the sustained release of VCM could kill the bacteria and prevent biofilm formation within 7 d.

Good Ti plays a crucial role in a Ti implant achieving an excellent osteointegration of the bone implant. The *in vitro* osteogenic properties of Tp and TV were found to be superior to that of T0, except for the expression of ALP at day 14. The ALP activity and ALP gene expression, as the early markers of osteogenic differentiation, were increased on Tp and TV. Also, enhanced bone formation and the late marker of osteogenic differentiation (OPN and OC) could be observed on the Tp and TV implant surfaces at 14 d. The improved osteogenic performance of Tp and TV could be attributed to the micro-patterned defined Ti implant, which could modulate the osteogenic differentiation of MSCs. The mico-patterned Ti coating could promote the cell adhesion and proliferation of BMSCs, which is crucial for osteogenic differentiation. On the other hand, the micro-patterned Ti coating can also promote the osteogenic differentiation of BMSCs. The results showed that the ALP activity in TV was not significantly higher than that of T0 at day 7 but was upregulated at day 14. We speculate that it may be

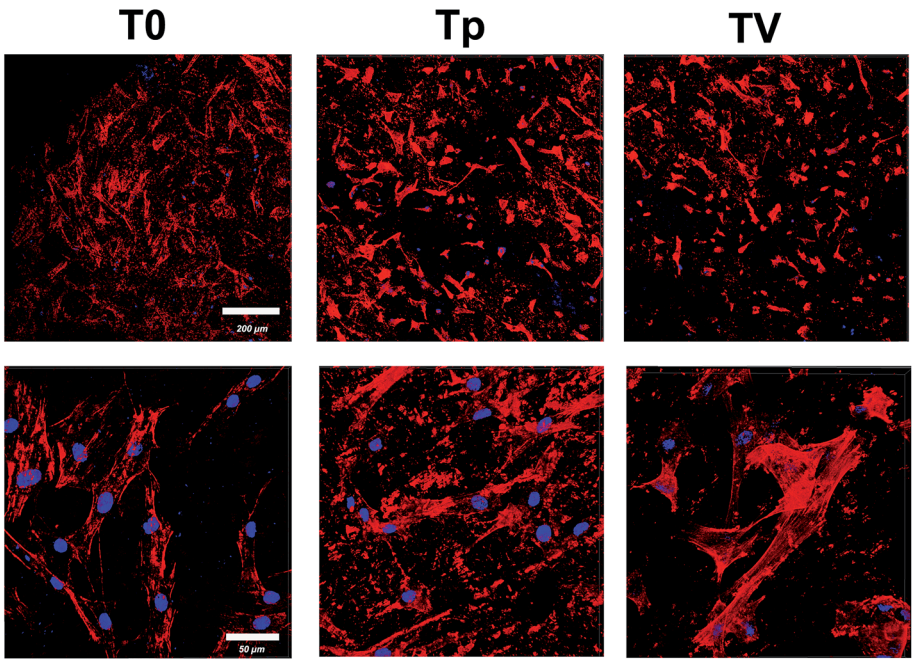

Fig. 8 Confocal laser scanning images of hBMSCs on the three samples (T0, Tp, and TV) stained with DAPI (blue) and rhodamine phalloidin (red) after 24 h culturing.

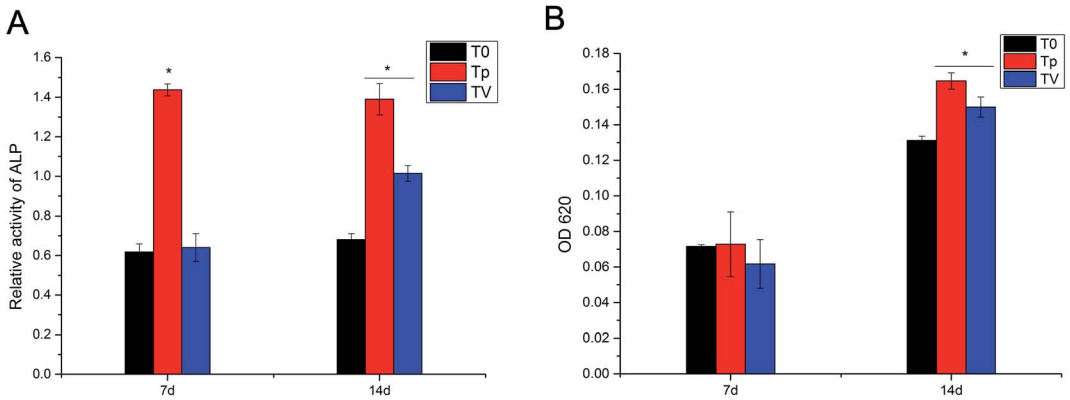

Fig. 9 Quantitative determination of the osteogenic differentiation of hBMSCs for all kinds of Ti substrates with ALP activity (A) and alizarin red staining (B). ALP activity in the Tp group was significantly higher than that of the other two groups at day 7, and the ALP activity in the Tp and TV groups was significantly higher than that of the T0 group at day 14; $*p < 0.05$. The quantitative mineralized nodule formation of Tp and TV was significantly higher than that of the ordinary T0 at day 14, indicating that Tp and TV could significantly promote the mineralization of ECM.

because of the release and effect of VCM on ALP, however, there are also studies reporting that VCM would not affect osteogenic differentiation at concentrations lower than 5000 μg mL^{-1},[32] thus it is necessary to carry out more investigations to gain deeper insights into the current results.

The surface properties of implants always influence the biocompatibility of Ti. For example, the nano-structured Ti surface can reduce the macrophage migration and activation, and different sizes of nano-topography on Ti can regulate the macrophage inflammatory response, thereby improving the osteointegration of the implant.[33] The micro-pattern with grid-like structure Ti can be doped by CPC with antibiotics for achieving the multi-biofunctionalization of Ti for anti-bacterial activity and promoting osteogenesis.

Thus, in this study, we designed coatings to prevent infection and promote bone mineralization, based on the regulation of the surface topography of the Ti implant combined with CPC–VCM doping on the Ti surface. They both exhibit independent advantages while not affecting each other. Our future studies will investigate whether this biological coating

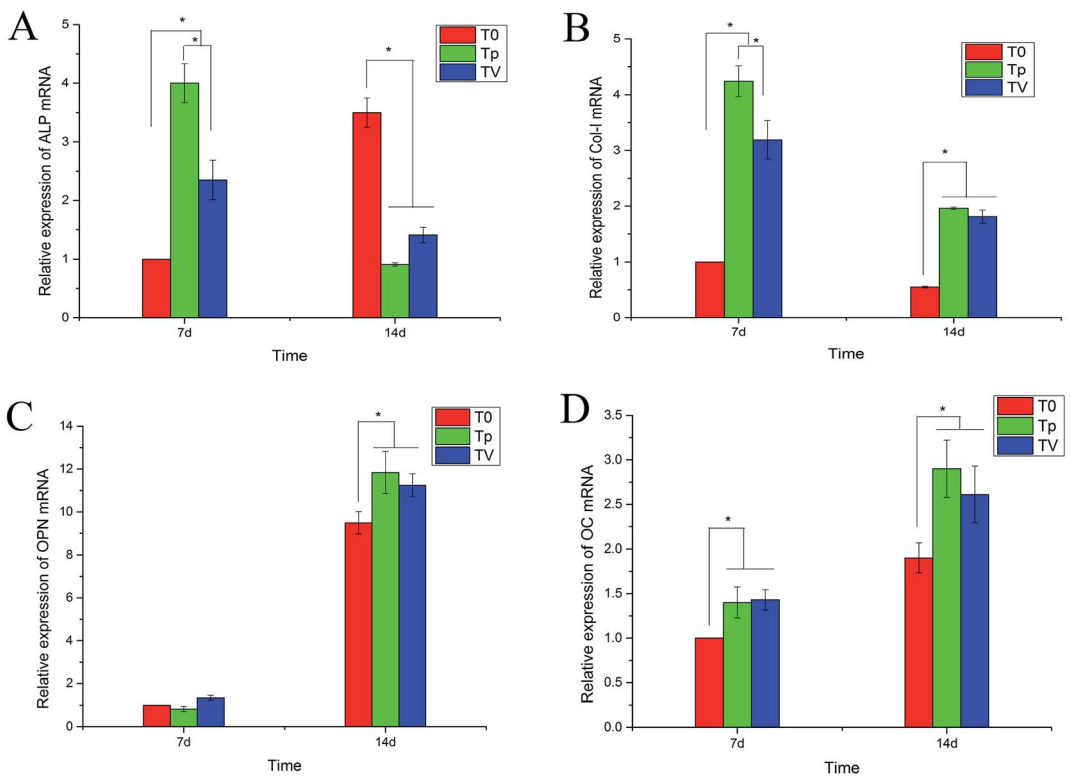

Fig. 10 Real-time PCR for the osteogenic gene expression of hBMSCs on various Ti substrates (T0, Tp and TV) under the conditions of the inducing osteogenic medium after 7 d and 14 d. (A) ALP, (B) COL1, (C) OPN and (D) OC; $*p < 0.05$.

continues to preserve the antibacterial activity and promote the bone-implant osteointegration properties *in vivo*.

Conclusion

To biofunctionalize Ti for improving the antibacterial property and enhancing the osteogenic activity, we introduced a micro-pattern coating on Ti. Furthermore, we doped CPC and VCM on the coating. The VCM–CPC doped in the micro-pattern coating on Ti could control the release of VCM for 6 d. The *in vitro* results showed that the antibacterial and osteogenic properties of the VCM–CPC doped on the micro-pattern coating improved. Our results demonstrated that this technique is a promising approach to biofunctionalize Ti for anti-bacterial activity and improving osteointegration.

Authors' contributions

Each author has contributed substantially to the research. All authors read and approved the final manuscript.

Authors' information

Guang-Chao Wang and Hao Zhang are co-first authors; Fang Ji and You-Tao Xie are co-corresponding authors.

Conflict of interest

The authors declare that they have no competing interests.

Availability of data and materials

The data is deposited in the Department of Orthopedics of Changhai Hospital. Please contact the corresponding author Fang Ji, doctorjif@126.com, for the usage of data.

Ethics approval and consent to participate

The subjects all gave their written informed consent in accordance with the Ethics Committee of Changhai Hospital.

Acknowledgements

This work was supported by grants from Shanghai Committee of Science and Technology Foundation (No. 13411951500).

References

1 L. A. Cordova, V. Stresing, B. Gobin, P. Rosset, N. Passuti, F. Gouin, V. Trichet, P. Layrolle and D. Heymann, *Clin. Sci.*, 2014, **127**, 277–293.
2 X. Liu, P. K. Chu and C. Ding, *Mater. Sci. Eng., R*, 2004, **47**, 49–121.
3 J. Cobo and J. L. Del Pozo, *Expert Rev. Anti-Infect. Ther.*, 2011, **9**, 787–802.
4 H. O. Gbejuade, A. M. Lovering and J. C. Webb, *Acta Orthopaedica*, 2015, **86**, 147–158.
5 D. A. Zubtsov, E. N. Savvateeva, A. A. Stomakhin, V. R. Chechetkin, A. S. Zasedatelev and A. Y. Rubina, *J. Biotechnol.*, 2009, **144**, 151–159.
6 S. Mantry, D. Behera, A. Satapathy, B. B. Jha and B. K. Mishra, *Surf. Eng.*, 2013, **29**, 222–227.
7 L. Zhao, H. Wang, K. Huo, L. Cui, W. Zhang, H. Ni, Y. Zhang, Z. Wu and P. K. Chu, *Biomaterials*, 2011, **32**, 5706–5716.
8 A. Zareidoost, M. Yousefpour, B. Ghaseme and A. Amanzadeh, *J. Mater. Sci.: Mater. Med.*, 2012, **23**, 1479–1488.
9 L.-H. Li, Y.-M. Kong, H.-W. Kim, Y.-W. Kim, H.-E. Kim, S.-J. Heo and J.-Y. Koak, *Biomaterials*, 2004, **25**, 2867–2875.
10 E. Kaivosoja, S. Myllymaa, Y. Takakubo, H. Korhonen, K. Myllymaa, Y. T. Konttinen, R. Lappalainen and M. Takagi, *J. Biomater. Appl.*, 2013, **27**, 862–871.
11 S. Fransiska, M. H. Ho, C. H. Li, J. L. Shih, S. W. Hsiao and D. V. H. Thien, *Biochem. Eng. J.*, 2013, **78**, 120–127.
12 Y. Shi, Y. Xie, H. Pan, X. Zheng, L. Huang, F. Ji and K. Li, *J. Therm. Spray Technol.*, 2016, 1–13.
13 S. B. Goodman, Z. Y. Yao, M. Keeney and F. Yang, *Biomaterials*, 2013, **34**, 3174–3183.
14 L. Zhao, P. K. Chu, Y. Zhang and Z. Wu, *J. Biomed. Mater. Res., Part B*, 2009, **91**, 470–480.
15 K. A. Poelstra, N. A. Barekzi, A. M. Rediske, A. G. Felts, J. B. Slunt and D. W. Grainger, *J. Biomed. Mater. Res.*, 2002, **60**, 206–215.
16 D. Loca, M. Sokolova, J. Locs, A. Smirnova and Z. Irbe, *Mater. Sci. Eng., C*, 2015, **49**, 106–113.
17 E. Vorndran, M. Geffers, A. Ewald, M. Lemm, B. Nies and U. Gbureck, *Acta Biomater.*, 2013, **9**, 9558–9567.
18 D.-J. Lin, C.-P. Ju, S.-H. Huang, Y.-C. Tien, H.-S. Yin, W.-C. Chen and J.-H. Chern Lin, *J. Mech. Behav. Biomed. Mater.*, 2011, **4**, 1186–1195.
19 B. e. Nie, H. Ao, C. Chen, K. Xie, J. Zhou, T. Long, T. Tang and B. Yue, *RSC Adv.*, 2016, **6**, 46733–46743.
20 D.-W. Lee, Y.-P. Yun, K. Park and S. E. Kim, *Bone*, 2012, **50**, 974–982.
21 B. e. Nie, H. Ao, J. Zhou, T. Tang and B. Yue, *Colloids Surf., B*, 2016, **145**, 728–739.
22 W. T. Lin, H. L. Tan, Z. L. Duan, B. Yue, R. Ma, G. He and T. T. Tang, *Int. J. Nanomed.*, 2014, **9**, 1215–1230.
23 U. Joosten, A. Joist, G. Gosheger, U. Liljenqvist, B. Brandt and C. von Eiff, *Biomaterials*, 2005, **26**, 5251–5258.
24 M. Stigter, G. K. De and P. Layrolle, *Biomaterials*, 2002, **23**, 4143–4153.
25 M. E. Bernardo, N. Zaffaroni, F. Novara, A. M. Cometa, M. A. Avanzini, A. Moretta, D. Montagna, R. Maccario, R. Villa, M. G. Daidone, O. Zuffardi and F. Locatelli, *Cancer Res.*, 2007, **67**, 9142.
26 J. Raphel, M. Holodniy, S. B. Goodman and S. C. Heilshorn, *Biomaterials*, 2016, **84**, 301–314.
27 Y.-Y. Guo, B. Liu, B.-B. Hu, G.-Y. Xiao, Y.-P. Wu, P.-F. Sun, X.-L. Zhang, Y.-H. Jia and Y.-P. Lu, *Surf. Coat. Technol.*, 2016, **294**, 131–138.

28 V. Antoci Jr, C. S. Adams, J. Parvizi, H. M. Davidson, R. J. Composto, T. A. Freeman, E. Wickstrom, P. Ducheyne, D. Jungkind, I. M. Shapiro and N. J. Hickok, *Biomaterials*, 2008, **29**, 4684–4690.
29 L. P. Actis, Dissertations & Theses – Gradworks, Ph.D., The University of Texas at San Antonio, 2014.
30 E. M. Hetrick and M. H. Schoenfisch, *Chem. Soc. Rev.*, 2006, **35**, 780–789.
31 V. T. Pham, V. K. Truong, A. Orlowska, S. Ghanaati, M. Barbeck, P. Booms, A. J. Fulcher, C. M. Bhadra, R. Buividas, V. Baulin, C. J. Kirkpatrick, P. Doran, D. E. Mainwaring, S. Juodkazis, R. J. Crawford and E. P. Ivanova, *ACS Appl. Mater. Interfaces*, 2016, **8**, 22025–22031.
32 C. R. Rathbone, J. D. Cross, K. V. Brown, C. K. Murray and J. C. Wenke, *J. Orthop. Res.*, 2011, **29**, 1070–1074.
33 Q. L. Ma, L. Z. Zhao, R. R. Liu, B. Q. Jin, W. Song, Y. Wang, Y. S. Zhang, L. H. Chen and Y. M. Zhang, *Biomaterials*, 2014, **35**, 9853–9867.